BER Analysis of a Novel Hybrid Modulation Scheme for Noncoherent DS-CDMA Systems

Dirk Nikolai and Karl-Dirk Kammeyer

University of Bremen, FB-1, Department of Telecommunications
P.O. Box 33 04 40, D-28334 Bremen, Germany
Tel.: ++(49)-421/218-2453, Fax: ++(49)-421/218-3341, E-mail: nikolai@comm.uni-bremen.de

ABSTRACT

A novel DS-CDMA transmission scheme combining the two well-known techniques of M-ary orthogonal and differential PSK-modulation is presented. This "hybrid" scheme is applicable to the noncoherent uplink of the IS-95 system where up to now only M-ary orthogonal modulation is used. The additional, PSK-modulated data show a slightly increased bit error rate (BER) compared to the data from M-ary modulation. However, the overall degradation caused hereby is far outweighed by the gain achieved by a higher spreading factor. Analytical results confirmed by simulations yield an improvement of approximately 1.0 dB in terms of $\bar{E}_b/N_0$ on a Rayleigh fading channel when no channel coding is used. This considerable gain is achieved upon only slight modification of the conventional modulation/demodulation procedure at a low additional complexity. It will be demonstrated that the IS-95 system is not properly designed since the full exploitation of noncoherent demodulation techniques results in a gain of nearly 2.0 dB.

1. INTRODUCTION

DIRECT SEQUENCE code division multiple access (DS-CDMA) is an attractive candidate to be considered for future mobile communication applications. In 1993, the standard IS-95, also called QUALCOMM-CDMA, was adopted in the USA [1]. Since then, much work has been carried out to improve IS-95 system performance by means of optimized demodulation techniques. In the asynchronous uplink, each user is received over different time-varying multipath radio channels at the common base station. This situation makes the optimum multiuser detection hardly feasible since the required channel estimation alone has a very high computational complexity. Furthermore, to meet the high accuracy requirements in channel parameter estimation, new channel estimation techniques have to be developed [2].

Even if only single-user detection is assumed, several approaches exist that lead to a better performance compared to the standard system. Among them are coherent demodulation techniques that require accurate channel estimates for each user separately, see e.g. [3]. Furthermore, "semicoherent" structures with poorer performance but less complex channel estimation procedures were investigated in [4] and [5]. In [6], an optimum metric for soft-bit Viterbi decoding was derived for the QUALCOMM-system exploiting the full information available in the *noncoherent* demodulation procedure.

In this paper, we introduce a novel hybrid modulation scheme designed for DS-CDMA systems exploiting both time resolution and complex signal space. With spread spectrum, the transmission symbols are multiplied by a high-rate pseudo-noise code. This increase in sampling rate can be used at least partly to perform an *encoding in time division*. For this, groups of $\log_2(M)$ bits choose one of M signal waveforms which differ in shape over time. An M-ary *orthogonal* modulation scheme is obtained by using Walsh functions for the signals – as employed in the QUALCOMM-system. The hybrid modulation procedure presented here extends the M-ary Walsh encoding by a differential phase-shift keying (DPSK). Due to the *differential* PSK, also the hybrid scheme becomes noncoherent and therefore keeps the system at a low complexity. This concept will be explained in detail in section 2.

Former investigations published in [7] show the bit error performance of hybrid modulation in an AWGN environment. In this paper, the bit error probability for transmission over Rayleigh fading channels is investigated in section 3. To underline the accuracy of the derivation, the analytical results are compared with simulation results. The paper will conclude with further simulations showing the performance of the described method in comparison to other proposals. It turns out that it is possible to achieve a gain of nearly 2.0 dB compared to the original proposal [8] even though the demodulation procedure is kept noncoherent.

2. SCHEME OF HYBRID MODULATION

The noncoherent transmission scheme used in the uplink of the IS-95 system [1, 8] is taken as a basis for the novel hy-

This research is supported by the German National Science Foundation (DFG-contract # Ka 841/4).
Compressed postscript files of our publications are available via `http://www.comm.uni-bremen.de`.

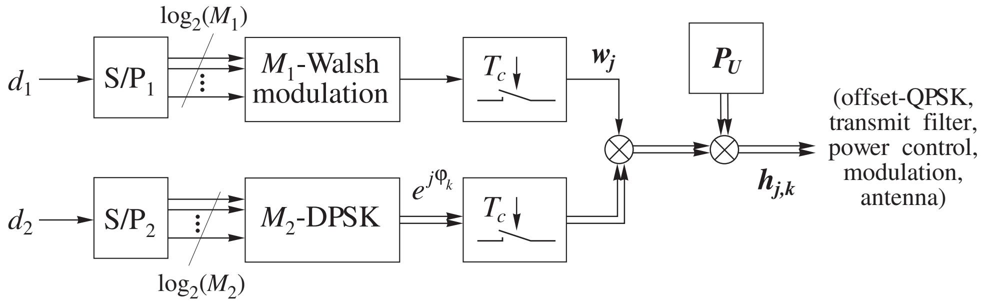

Figure 1: Hybrid modulation scheme.

brid modulation scheme described in this paper. The conventional scheme is shown in the upper branch of **figure 1** for the general case of M_1-ary orthogonal modulation. The data d_1 serving as the input for the upper branch may already be convolutionally encoded. In each modulation interval, $K_1 = \log_2(M_1)$ binary symbols are grouped together and choose one of M_1 corresponding real valued Walsh symbols

$$\boldsymbol{w}_j = \left[\, w_j(0), \ldots, w_j(M_1-1)\,\right]^T, \; j \in \{0, \ldots, M_1-1\},$$

(vector representation) with components $w_j(\nu) \in \{-1, 1\}$. Such a binary vector can be easily generated from Walsh functions, known as Hadamard matrices in their discrete representation. The complete set of M_1 Walsh symbols represents an orthogonal basis satisfying the condition

$$\boldsymbol{w}_i^* \, \boldsymbol{w}_j \;=\; M_1 \, \delta_{ij} \;,$$

where the superscript "$*$" denotes a vector *transjugation*, i.e. the complex conjugation of vector elements including the vector transpose, which will turn out to be useful in the case of complex signals. Since $w_j(\nu) \in \{-1, 1\}$, M_1 represents the symbol energy, and δ_{ij} is the Kronecker symbol. In the IS-95 uplink, the M_1-ary Walsh symbols with $M_1 = 64$ are further spread by a factor of 4 due to the multiplication with a user specific code $P_U(k)$ of rate $1/T_c$ ("chip rate") that performs the multiple access. This code is a complex valued pseudo-random noise sequence ("PN sequence") that, besides the user separation, also introduces a so-called "quadrature spreading" which prepares an offset QPSK following the stages shown in figure 1. After multiplication, we obtain the transmission symbols $\boldsymbol{h}_j = \boldsymbol{P}_U \, \boldsymbol{w}_j$ of length $N_s = 4 \cdot M_1$, where $\boldsymbol{P}_U$ denotes an appropriate matrix containing the corresponding part of $P_U(k)$. Of course, the PN spreading does not affect the orthogonality of the transmission symbols:

$$\begin{aligned} \boldsymbol{h}_i^* \, \boldsymbol{h}_j &= (\boldsymbol{P}_U \, \boldsymbol{w}_i)^* \; \boldsymbol{P}_U \, \boldsymbol{w}_j \\ &= \boldsymbol{w}_i^* \; \underbrace{\boldsymbol{P}_U^* \boldsymbol{P}_U}_{\text{identity matrix}} \; \boldsymbol{w}_j \;=\; N_s \, \delta_{ij} \;. \end{aligned}$$

For hybrid modulation, we just perform a phase modulation of the real valued Walsh symbols before spreading, as shown in figure 1. Here, each Walsh symbol $\boldsymbol{w}_j$ is multiplied by a constant phase shift $e^{j\varphi_k}$ determined by $K_2 = \log_2(M_2)$ bits (d_2 in the lower branch) yielding the *hybrid symbols* $\boldsymbol{h}_{j,k}$. This process is illustrated at the top of **figure 2**. Each real valued Walsh symbol is phase-shifted according to $e^{j\varphi_k}$. Due to the following complex PN spreading, the signal becomes complex anyway, regardless whether the input was real valued (as in the nonhybrid conventional case) or complex as in the hybrid case shown in the figure.

Although not mandatory, the phase modulation should be carried out in its *differential* form (M_2-DPSK) to make a noncoherent detection possible.

To illustrate the influence of a radio channel on the hybrid symbols, we assume a multipath channel model consisting of L complex multiplicative factors c_λ (i.e. amplitude and phase shift) and additive noise $\boldsymbol{r}_\lambda$, which models both the thermal noise and the multiple access interference in the CDMA environment. The elements of $\boldsymbol{r}_\lambda$ can be regarded as uncorrelated Gaussian stochastic variables with power σ_r^2 each. With this, the received signal on the λ-th echo path, $\lambda \in \{0, \ldots, L-1\}$, is

$$\boldsymbol{s}_\lambda \;=\; c_\lambda \, \boldsymbol{h}_{j,k} + \boldsymbol{r}_\lambda \;=\; c_\lambda \, e^{j\varphi_k} \, \boldsymbol{h}_j + \boldsymbol{r}_\lambda \;.$$

At the receiver, the incoming signals $\boldsymbol{s}_\lambda$ are despread with the user-specific complex conjugate PN sequence $\boldsymbol{P}_U^*$, see **figure 3**, and summed up over 4 times the chip duration. Then, the signals are correlated with all M_1 hypotheses of transmission symbols $\boldsymbol{w}_i$, carried out efficiently by the discrete Hadamard transform (DHT). In our notation, these steps are simplified to the correlation with all possible symbols $\boldsymbol{h}_i$. With square law detection – shown in the upper branch of figure 3 – we obtain for the M_1 correlations:

$$\begin{aligned} V_i^{(\lambda)} = |\boldsymbol{h}_i^* \boldsymbol{s}_\lambda|^2 &= |\boldsymbol{h}_i^* \, c_\lambda \, e^{j\varphi_k} \boldsymbol{h}_j + \boldsymbol{h}_i^* \, \boldsymbol{r}_\lambda|^2 \\ &= |\boldsymbol{h}_i^* c_\lambda e^{j\varphi_k} \boldsymbol{h}_j|^2 + 2\,\mathrm{Re}\{\tilde{r}_\lambda\} + |\boldsymbol{h}_i^* \boldsymbol{r}_\lambda|^2 \\ &= \underbrace{|e^{j\varphi_k}|^2}_{\equiv 1} \cdot \, |c_\lambda \, N_s \delta_{ij}|^2 \;+\; n_\lambda \;, \end{aligned} \qquad (1)$$

where the noise terms $\tilde{r}_\lambda = \boldsymbol{h}_i^* \, c_\lambda \, e^{j\varphi_k} \boldsymbol{h}_j \boldsymbol{r}_\lambda^* \boldsymbol{h}_i$ and $|\boldsymbol{h}_i^* \boldsymbol{r}_\lambda|^2$ have been combined in n_λ. The term $\boldsymbol{h}_i^* \, \boldsymbol{r}_\lambda$ represents a complex stochastic white process with variance $N_s \sigma_r^2$. As can be seen from eq. (1), the phase modulation $e^{j\varphi_k}$ – having a constant envelope – is without any influence on the conventional noncoherent demodulation procedure for the Walsh symbols. Hence, eq. (1) reduces to an expression equivalent to the one obtained in the conventional (nonhybrid) case, i.e. $|c_\lambda \, N_s \delta_{ij}|^2$ and additive noise. Due to the multipath propagation, the correlations are carried out in more than one branch of the RAKE receiver, denoted as "further RAKE fingers" in figure 3. The maximum likelihood receiver detects the value with maximum magnitude of the M_1 decision components

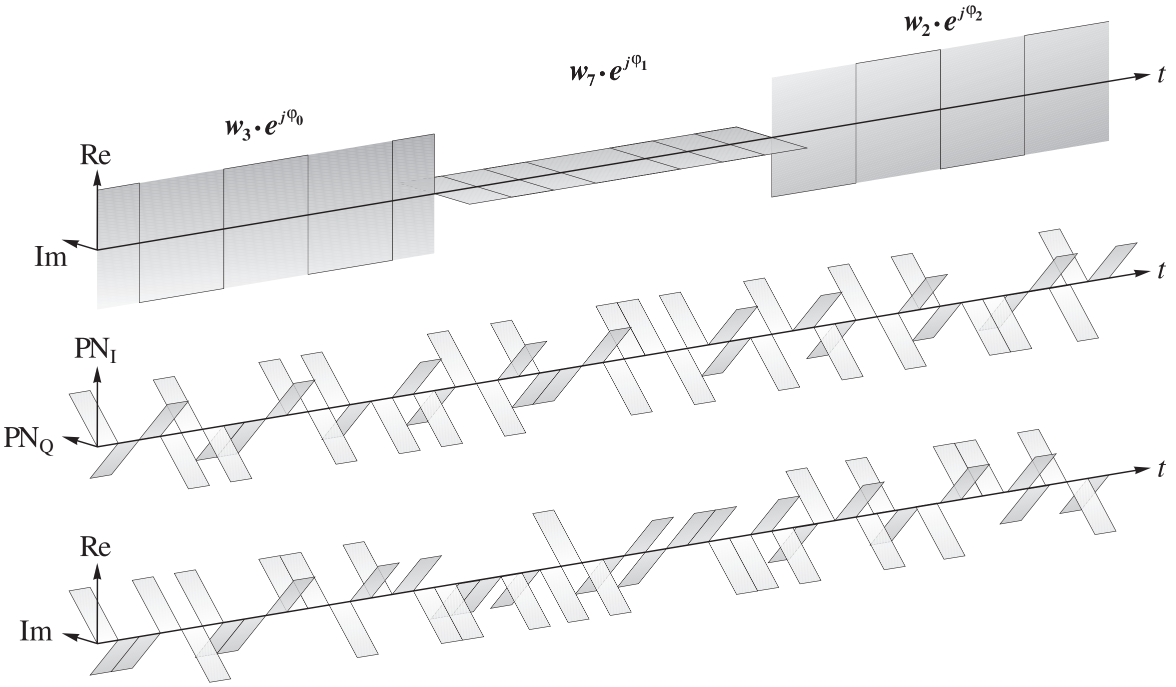

Figure 2: Hybrid symbols, complex spreading sequence and signal to be transmitted.

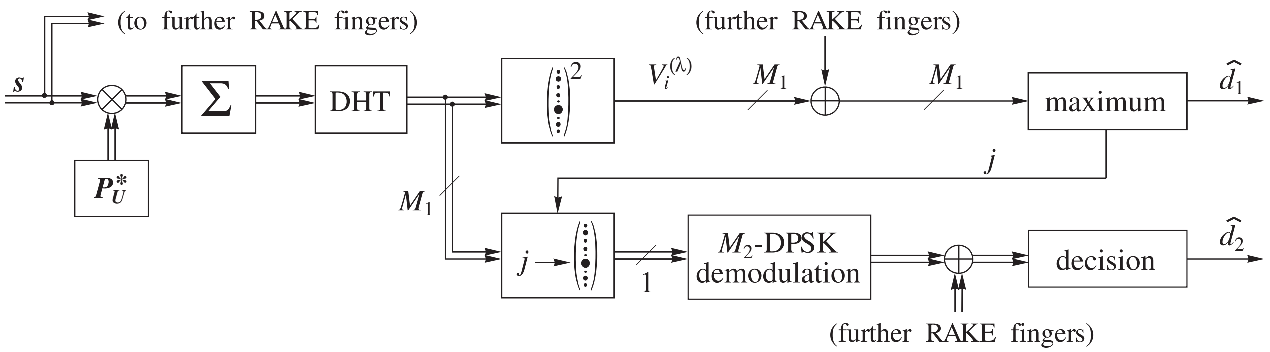

Figure 3: Noncoherent hybrid demodulation scheme (one RAKE branch).

calculated according to

$$\hat{V}_j \;=\; \max_{(i)} \sum_{\lambda=0}^{L-1} V_i^{(\lambda)} \,. \tag{2}$$

The index of this value indicates the most likely transmitted Walsh symbol leading to the data $\hat{d}_1$ [9]. Next, the additional data transmitted with $e^{j\varphi_k}$ are obtained by detecting the phase difference between two consecutively decided (non-squared and hence complex) symbols, as depicted in the lower branch of figure 3, finally leading to $\hat{d}_2$.

3. BIT ERROR PERFORMANCE FOR DPSK WITH *L*-PATH RAYLEIGH FADING

Due to the hybrid modulation described in the former section, we have to distinguish between two types of binary data: on the one hand, at any one time K_1 bits belonging to the Walsh part of each hybrid symbol and on the other hand, K_2 bits belonging to the DPSK part. In the following, they will be called "Walsh-bits" and "DPSK-bits", respectively.

To give an expression for the Walsh-bit error probability in case of an L-path Rayleigh channel, we start with the error probability of the *Walsh symbols* which is in case of noncoherent detection (e.g. [9, 10])

$$P_{s,Walsh} \;=\; 1-\int_0^\infty \frac{v^{L-1}}{(L-1)!\,(1+\bar{\gamma}_c)^L} \cdot e^{-\frac{v}{1+\bar{\gamma}_c}} \left(1-e^{-v}\sum_{\lambda=0}^{L-1}\frac{v^\lambda}{\lambda!}\right)^{M_1-1} dv \tag{3}$$

with $\bar{\gamma}_c = \frac{1}{L}\frac{\bar{E}_S}{N_0} = \frac{K_1}{L}\frac{\bar{E}_b}{N_0}$ as the average SNR per path of the Rayleigh channel. From eq. 3, the error probability of the corresponding *Walsh-bits* is calculated according to

$$P_{b,Walsh} \;=\; \frac{M_1/2}{M_1-1}\cdot P_{s,Walsh}\,, \tag{4}$$

where the last equation holds for equiprobable orthogonal signals [9].

In contrast, the error probability of the additional DPSK-bits is

$$P_{b,DPSK}^{(hybrid)} \;=\; \frac{1}{2}\cdot(1-P_2) \;+\; P_{b,DPSK}^{(M_2)}\cdot P_2\,. \tag{5}$$

Here, P_2 denotes the *probability that two consecutive Walsh symbols are decided correctly*. Even if this happens, the differentially phase-encoded bits may nonetheless be false due to noise. For this, the probability P_2 has to be multiplied with the corresponding expression for $P_{b,DPSK}^{(M_2)}$ describing the conventional DPSK bit error probability, as performed in the second term in eq. (5). For example, in case of $M_2 = 4$ (DQPSK), and Gray encoded data d_2, we have to take [9]

$$P_{b,DPSK}^{(M_2=4)} = \frac{1}{2} - \frac{\mu/2}{\sqrt{2-\mu^2}} \sum_{\lambda=0}^{L-1} \binom{2\lambda}{\lambda} \left(\frac{1-\mu^2}{4-2\mu^2}\right)^{\lambda} \quad (6)$$

with $\mu = \frac{\bar{\gamma}_c}{1+\bar{\gamma}_c}$.

The first term in eq. (5) follows from the fact that even if false Walsh symbols are detected, which occurs with probability $(1 - P_2)$ (no matter whether both involved symbols or only one of them is false), still in $1/M_2$ of all cases a DPSK-symbol is detected correctly by chance. It follows that a *false* detection occurs with probability $1 - 1/M_2$. Although eq. (4) is originally valid for equiprobable orthogonal signals, the equation is as well applicable to the case considered here: if at least one Walsh symbol is false, all corresponding *phases* become equiprobable – the Gray encoding is insignificant here. So, only part of the binary symbols are false, which finally results in

$$\left(1 - \frac{1}{M_2}\right) \cdot \frac{M_2/2}{M_2-1} = \frac{1}{2}\,, \quad (7)$$

which is the factor appearing in eq. (5).

The required expression for P_2 in eq. (5) turns out to be a little sophisticated and will be derived in a step-by-step manner. The probability density function (pdf) of V_j in eq. (2) is for an L-path channel in case of a correct hypothesis [9]

$$p(V_j|\boldsymbol{h}_j) = \frac{1}{\sigma^2}\left(\frac{V_j}{\varrho^2}\right)^{\frac{L-1}{2}} e^{-\frac{(V_j+\varrho^2)}{\sigma^2}}\, I_{L-1}\left(\frac{2\,\varrho\sqrt{V_j}}{\sigma^2}\right), \quad (8)$$

which is a noncentral chi-square pdf with $2L$ degrees of freedom with $\sigma^2 = N_s \cdot \sigma_r^2$. $I_{L-1}(\cdot)$ denotes the $(L-1)$-th order modified Bessel function of the first kind. For a fixed channel fading situation, the noncentrality parameter ϱ^2 is given as

$$\varrho^2 = \sum_{\lambda=0}^{L-1} |c_\lambda \cdot N_s|^2 = N_s^2 \sum_{\lambda=0}^{L-1} |c_\lambda|^2\,. \quad (9)$$

The remaining $M_1 - 1$ correlation results show a central chi-square pdf:

$$p(V_i|\boldsymbol{h}_j) = \frac{1}{\sigma^{2L}(L-1)!}\, e^{-\frac{V_i}{\sigma^2}}\, V_i^{L-1}\,, \quad i \neq j\,. \quad (10)$$

The probability of a correct Walsh symbol decision is the probability that V_j exceeds the $M_1 - 1$ other results. The probability that V_j is greater than any other V_i is calculated according to [9]

$$P(V_i < V_j) = \int_0^{V_j} p(V_i|\boldsymbol{h}_j)\, dV_i = 1 - e^{-\frac{V_j}{\sigma^2}} \sum_{\lambda=0}^{L-1} \frac{1}{\lambda!}\left(\frac{V_j}{\sigma^2}\right)^{\lambda}. \quad (11)$$

Since the $M_1 - 1$ correlation results are statistically independent, eq. (11) has to be multiplied (M_1-1)-fold to obtain the required probability. The resulting expression has to be averaged over the pdf of V_j for a fixed value of ϱ^2 to obtain the probability of a correct Walsh symbol decision:

$$P_c(\varrho^2) = \int_0^{\infty} p(V_j|\boldsymbol{h}_j) \cdot \left(P(V_i < V_j)\right)^{M_1-1} dV_j\,. \quad (12)$$

In the following, we assume a sufficiently slowly fading channel, i.e. c_λ and hence ϱ^2 are constant over the duration of two hybrid symbols. Due to statistically independent symbol decisions at a fixed fading situation, we simply have to square eq. (12) to obtain the probability of *two* consecutive correct symbols. The averaging over the pdf of the noncentrality ϱ^2, which is

$$p(\varrho^2) = \frac{1}{\sigma_\varrho^{2L}\,(L-1)!} \cdot e^{-\frac{\varrho^2}{\sigma_\varrho^2}} \cdot \varrho^{2(L-1)} \quad (13)$$

with $\sigma_\varrho^2 = \sigma^2\bar{\gamma}_c$, finally leads to the required expression

$$P_2 = \int_0^{\infty} p(\varrho^2) \cdot P_c^2(\varrho^2)\, d\varrho^2\,. \quad (14)$$

The evaluation of eq. (5) by numerical integration of eq. (14) yields the results shown in the upper solid curve of **figure 4** in case of a 4-path Rayleigh channel. All curves show analytical results, whereas the circles stem from simulations. The middle solid curve is obtained by averaging the probabilities in eq. (4) and eq. (5) according to

$$\bar{P} = \frac{K_1 \cdot P_{b,Walsh} + K_2 \cdot P_{b,DPSK}^{(hybrid)}}{K_1 + K_2}\,. \quad (15)$$

The mean error probability $\bar{P}$ of all transmitted bits has to be compared with the error probability obtained in the conventional case, which is represented by the dashed line. The comparison of both curves yields a gain of approximately 1.0 dB for the novel hybrid scheme.

Care should be taken to the fact that all analytical curves offer a lower bit error probability than the corresponding simulation results due to the non-ideal correlation properties of

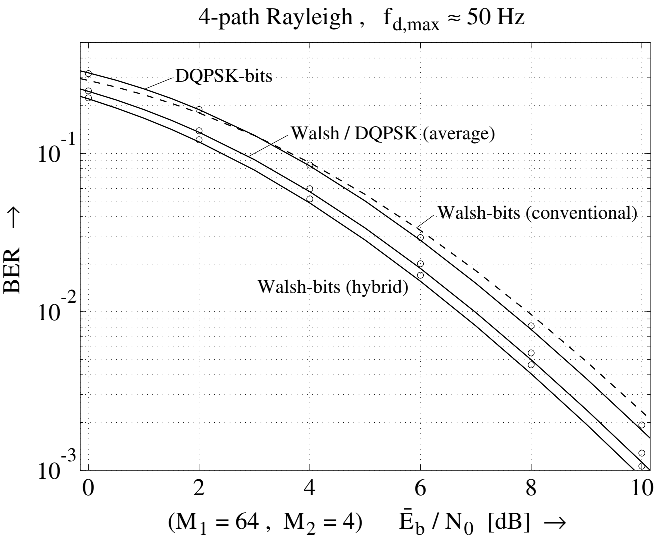

Figure 4: BER for hybrid modulation with DQPSK: analytical (–) and simulation (○) results (without channel coding).

the PN long-code. This causes self-interference which is yet neither considered in eq. (4) for the Walsh-bits nor in eq. (5) for the DPSK-bits.

4. DISCUSSION

The hybrid modulation technique developed in this paper allows the transmission of additional data in a noncoherent DS-CDMA communication system at a slightly increased error rate – without interfering with the original, non-hybrid system. The "additional" data d_2 may come from the same source as the data d_1 transmitted with the Walsh symbols. Such a concept can be realized using a demultiplexer $K_1 : K_2$ at the transmitter and a corresponding multiplexer at the receiver.

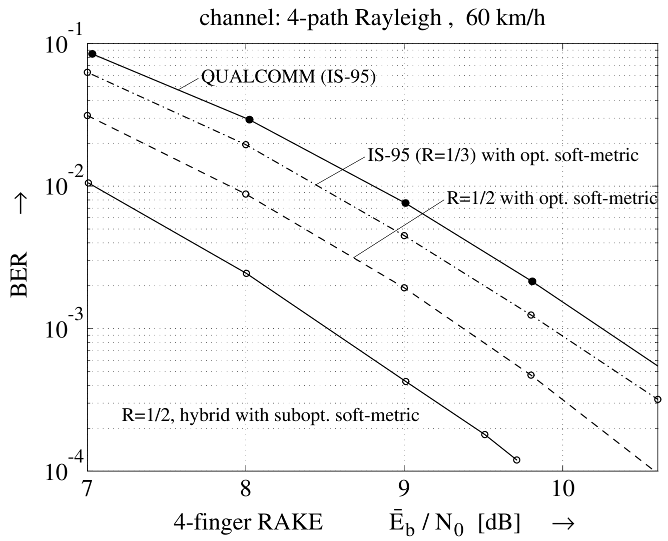

Figure 5: BER of hybrid modulation scheme (lower curve) including convolutional encoding in comparison with QUALCOMM (upper curve) and others (simulation results).

First simulation results including channel encoding with soft-bit decoding at the receiver are shown in **figure 5** for various detection methods. The optimum exploitation of soft-bit information introduced in [6] yields a gain of approximately 0.3 dB compared to the QUALCOMM system shown in the upper curve. Optimizations published in [11] show a better performance of the system when a code rate of $R = 1/2$ instead of $R = 1/3$ is used. For the case considered in figure 5, we get an additional gain of nearly 0.5 dB. A further decrease of the bit error probability is possible with hybrid modulation. Here, the gain turns out to be nearly 1.0 dB, which is a considerable quantity compared to the other improvements. This gain is achieved using an until now suboptimum soft-decision metric for the DPSK-bits (i.e. $\hat{d}_2$).

It should be emphasized that all improvements shown in figure 5 are achieved still using noncoherent demodulation techniques. Hence, a rather simple receiver structure is assumed in any case. Figure 5 shows that the IS-95 system is not properly designed since the full exploitation of noncoherent demodulation techniques results in a gain of 1.8 dB.

5. REFERENCES

[1] TIA/EIA Interim Standard IS-95. *Mobile Station - Base Station Compatibility Standard for Dual-Mode Wideband Spread Spectrum Cellular System.* Telecommunications Industry Association, July 1993.

[2] J. Panicker and S. Kumar. Effect of System Imperfections on BER Performance of a CDMA Receiver with Multipath Diversity Combining. *IEEE Trans. on Vehicular Technology*, 45(4):622–630, November 1996.

[3] P. Schramm and J. Huber. Coherent Demodulation for IS-95 Uplink. In *Proc. IEEE Int. Symposium on Spread Spectrum Techniques & Applications (ISSSTA)*, volume 3, pages 1073–1077, Mainz, Germany, September 22-25 1996.

[4] P. Schramm. Attractive Coded Modulation Schemes for the Uplink in CDMA-Mobile Communication Systems. In *ITG-Fachbericht Mobile Kommunikation*, volume 135, pages 255–262, Neu-Ulm, Germany, September 26-28 1995. VDE Verlag.

[5] D. Nikolai and K.D. Kammeyer. Noncoherent RAKE-Receiver with Optimum Weighted Combining and Improved Closed-Loop Power Control. In *Proc. IEEE Int. Symposium on Spread Spectrum Techniques & Applications (ISSSTA)*, volume 1, pages 239–243, Mainz, Germany, September 22-25 1996.

[6] M. Benthin and K.D. Kammeyer. Viterbi Decoding of Convolutional Codes with Reliability Information for a Noncoherent RAKE-Receiver in a CDMA-Environment. In *Proc. IEEE Global Telecommun. Conf. (GLOBECOM)*, pages 1758–1762, San Francisco, USA, November 28 - December 2 1994.

[7] K.D. Kammeyer and D. Nikolai. A New CDMA-Concept using Hybrid Modulation with Noncoherent Detection. In *Proc. IEEE Fourth Symposium on Commun. and Vehicular Technology in the Benelux (SCVT'96)*, pages 102–107, Gent, Belgium, October 7-8 1996.

[8] A.J. Viterbi, A.M. Viterbi, and E. Zehavi. Performance of Power-Controlled Wideband Terrestrial Digital Communication. *IEEE Trans. on Communications*, 41(4):559–569, April 1993.

[9] J.G. Proakis. *Digital Communications*. McGraw-Hill, third edition, 1995.

[10] K.D. Kammeyer. *Nachrichtenübertragung*. B.G. Teubner, Stuttgart, second edition, 1996.

[11] M. Bickel, W. Granzow, and P. Schramm. Optimization of Code Rate and Spreading Factor for Direct–Sequence CDMA Systems. In *Proc. IEEE Int. Symposium on Spread Spectrum Techniques & Applications (ISSSTA)*, volume 2, pages 585–589, Mainz, Germany, September 22–25 1996.